Long-term survival of the axial valley morphology at abandoned slow-spreading centers

Andrew M. Freed Department of Geosciences, University of Arizona, Tucson, Arizona 85721
Jian Lin, Peter R. Shaw Woods Hole Oceanographic Institution, Woods Hole, Massachusetts 02543
H. Jay Melosh Lunar and Planetary Laboratory, University of Arizona, Tucson, Arizona 85721

ABSTRACT

Results of a lithospheric stretching model of mid-ocean ridges suggest that the axial valley topography created at active slow-spreading centers may be preserved for tens of millions of years after cessation of spreading. We simulate the evolution of a slow-spreading center using a finite-element model that incorporates a temperature-dependent rheology and discrete faulting. Model results show that significant valley morphology persists after regional extension ceases because the high lithospheric viscosities associated with a slow-spreading center prevent ductile relaxation and because no effective mechanism exists to reverse rift-bounding normal faults. Removal of the axial valley can only be accomplished by reversal of the regional extensional strains immediately upon cessation of active spreading. However, such a process does not seem likely. These results suggest that the persistence of axial valleys at extinct spreading centers is consistent with a lithospheric stretching model for active slow-spreading ridges.

INTRODUCTION

Slow-spreading mid-ocean ridges (10–50 mm/yr) such as the Mid-Atlantic Ridge (Fig. 1a) are characterized by a prominent axial valley 10–40 km wide and 1–3 km deep (e.g., Macdonald, 1982). Evidence from gravity (Collete et al., 1980; Parmentier and Forsyth, 1985; Lin et al., 1990; Blackman and Forsyth, 1991) and seismic (Purdy and Detrick, 1986; Louden et al., 1986) studies at active ridges indicate a uniform cross-axis crustal thickness, suggesting that this valley is not supported by Airy isostasy. These observations are consistent with the idea of lithospheric stretching as the cause of an axial valley (e.g., Tapponier and Francheteau, 1978). The lithospheric stretching mechanism could be formulated as a bending moment produced by horizontal extension in a plastic plate that thickens with distance from a ridge axis (Phipps Morgan et al., 1987; Lin and Parmentier, 1989; Chen and Morgan, 1990; Neumann and Forsyth, 1993; Phipps Morgan and Chen, 1993). Alternatively, the stretching could be accomplished by formation of successive rift-bounding normal faults that are rotated by isostatic plate flexure as they move away from the ridge axis (Shaw and Lin, 1993).

It is not clear, however, how the dynamic mechanism of lithospheric stretching can quantitatively explain the preservation of prominent axial valleys at extinct spreading centers, where extension has long ceased. In other words, when the regional strain rate vanishes, would the lithosphere relax enough to allow isostatic forces to remove a significant portion of the axial valley? Abandoned centers can be found in many locations, including the Labrador (Osler and Louden, 1995), Coral, and Scotia seas (cf. Jonas et al., 1991), the Pacific Ocean (Batiza and Chase, 1981), the Indian Ocean (Small and Sandwell, 1994), and on the African plate east of the Mid-Atlantic Ridge near lat 40°–50°S (Fig. 1b). Here we present a quantitative analysis of the evolution of an abandoned spreading center to examine whether the creation of an axial valley by lithospheric stretching is a reversible or irreversible process.

MODEL

We study the interplay between lithospheric stretching accommodated by discrete faults and asthenospheric stress relaxation using a time-dependent, viscoelastic, finite-element model (Melosh and Raefsky, 1981). The two-dimensional, finite-element model spans a sufficiently long distance (300 km) from the spreading axis and great depth (150 km) beneath the sea floor to minimize the influence of far field conditions on ridge-axis processes. Assumed symmetry about the ridge-axis ($x = 0$) allows us to model only one side of the ridge (Fig. 2). Our rheology is based on an across-axis temperature profile midway between the center and distal end of a 50-km-long segment at a slow-spreading ridge with a half-rate of 12 mm/yr (from our three-dimensional thermal model of Shaw and Lin). The model has a 5-km-thick crust (Young's modulus $E_c = 8 \times 10^{10}$ N/m^2, Poissons ratio $\nu_c = 0.25$, density $\rho_c = 2900$ kg/m^3) over a mantle half-space ($E_m = 11 \times 10^{10}$ N/m^2, $\nu_m = 0.25$, $\rho_m = 3300$ kg/m^3). Viscosities are based on experimentally determined flow laws, $\dot{e} = A\ \sigma^n \exp(-Q/RT)$, where $\dot{e}$ is the strain rate, A is the flow-law constant, σ is the differential stress, n is the power law, Q is the activation energy, R is the gas constant, and T is the absolute temperature. Crustal viscosities are based on $A_c = 10^2$ (MPa)^n s^{-1}, $n_c = 3.4$, and $Q_c = 260$ kJ/mol, and mantle viscosities are based on $A_m = 10^3$ (MPa)^n s^{-1}, $n_m = 3.0$, and $Q_m = 450$ kJ/mol. These values are from Kirby (1983), except for Q_m, for which a smaller value was chosen to allow the base of the mechanical lithosphere to coincide with the 750 °C isotherm.

Seismic moment studies of Solomon et al. (1988) show that 10%–20% of sea-floor spreading at a slow-spreading ridge is accommodated by extensional faulting and the rest by magmatic emplacement. In this study we assume a lithospheric stretching rate, V_{ext}, that equals 20% of the half-spreading rate, V_o. In the cyclic faulting model of Shaw and Lin, only the innermost rift-bounding fault is active and extends from the sea floor to the base of the lithosphere (Fig. 2). This model is self consistent in the calculated thermo-mechanical structure and fault kinematics. Assuming that active faulting occurs on a plane that minimizes the resistance due to cohesive, frictional, and plate flexural forces, Shaw and Lin have obtained a steady-state solution of cyclic faulting. For the rheological structure of Figure 2, the solution requires that each active fault initiates at distance $x_i = 8$ km from the ridge axis at the beginning of a faulting cycle ($t_i = 0$) and increases slip to $s_{max} = 1$ km by the end of cycle ($t_f = 0.4$ m.y.) when the fault has traversed $\Delta x = 5$ km to a location $x_f = x_i + \Delta x = 13$ km from the ridge axis. Outboard of the active fault, dormant faults are predicted at $\Delta x = 5$ km intervals with successive block rotation of up to $\Delta\theta = 9°$ (Shaw and Lin, 1993) (Fig. 2). This cyclic faulting model is consistent with seismic data at the Mid-Atlantic Ridge, which indicate that active faulting is contained primarily within the flanking highs that bound the axial valley (Toomey et al., 1988; Lin and Bergman, 1990).

We modeled the active fault by utilizing slippery nodes that allow frictionless sliding between adjacent elements along a predetermined fault plane (Melosh and Williams, 1989). The spreading

Figure 1. Marine free-air gravity of southern Atlantic as viewed from combined GEOSAT and other satellite data (Sandwell and Smith, 1992). Free-air gravity reflects primarily topographic effects. Illumination is from east. a: Active segment of slow-spreading Mid-Atlantic Ridge (half-spreading rate = ~17 mm/yr). Spreading axis is denoted by valley topography typical of active slow-spreading centers. b: Extinct spreading center trends north-south at long 15 °E. This abandoned spreading center is due east of Mid-Atlantic Ridge and has negative free-air gravity similar to that of active center. Inset: Comparison of gravity profiles across active (solid line) and extinct (dotted line) axial valleys.

Figure 2. Upper left part of finite-element model used to study processes that lead to axial valley at active slow-spreading center. Moho shows previously broken and rotated crust. Innermost fault is free to slip. Viscosities used in model are temperature dependent and based on experimental flow laws (see text). Effective viscosities (for display purposes only) assume strain rate of 10^{-15} s^{-1}. Base of mechanical lithosphere is denoted by 750 °C isotherm. Full model is 300 km wide and 150 km deep.

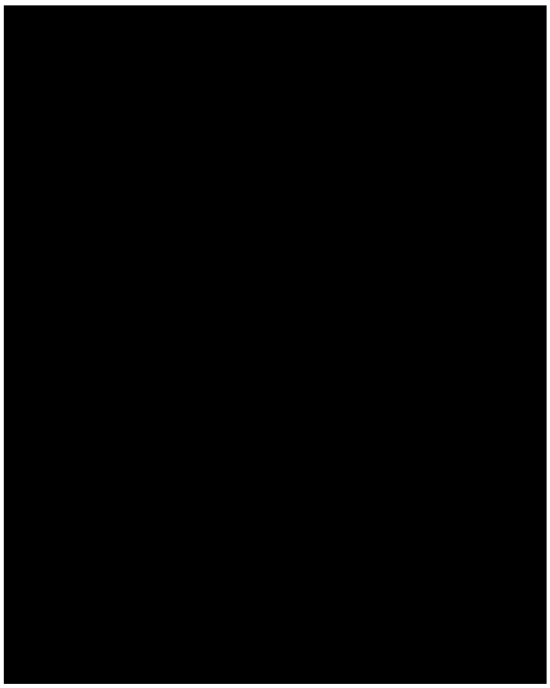

Figure 3. a: Predicted deformation and horizontal deviatoric stress field, $\sigma_x - P$, where $P = (\sigma_x + \sigma_y + \sigma_z)/3$, for active slow-spreading center. Note effect of plate bending as revealed by extensional stresses (red) overlying compressional stresses (blue) in region of inner valley ($x < 15$ km), and compression overlying extension in region of flanking mountains ($x > 20$ km). b: Predicted deformation and horizontal deviatoric stress field for 40 m.y. old abandoned slow-spreading center. Note that overall morphology and state of stress of extinct spreading center is little changed from active center.

axis ($x = 0$) is fixed horizontally, but free to displace vertically. Appropriate horizontal stretching rates are applied to the lithosphere on the right side of the model ($x = 300$ km) to simulate active and extinct centers, respectively (see discussion in next section). To conserve mass within the model box, a parabolic counterflow is applied to the asthenosphere along the right boundary. This counterflow is equivalent to the return flow described by kinematic models of upper mantle circulation (Chase, 1979; Parmentier and Oliver, 1979). The bottom of the model (at a depth of 150 km) is fixed vertically. The model also takes into account pressure from a 3 km water column, gravity body force, and assumes an initial lithostatic state of stress.

RESULTS

For the cyclic faulting model associated with the configuration of Figure 2, we have calculated the corresponding stress distribution in the crust and mantle. Figure 3a shows the axial valley topography and the associated horizontal deviatoric stress, $\sigma_x - P$, where $P = (\sigma_x + \sigma_y + \sigma_z)/3$, at the end of a faulting cycle of a steady-state active spreading center. The stress field is controlled primarily by plate bending associated with isostasy and regional extension associated with stretching. Because these quantities do not vary significantly during a faulting cycle, the solution shown in Figure 3a can be considered as a first-order approximation of steady-state stresses. The main features in the stress field are as follows. (1) Deviatoric stresses below the 750 °C isotherm are insignificant except directly beneath the active fault where local strain rates are high. This demonstrates that the base of the mechanical lithosphere coincides with the 750 °C isotherm in our model. (2) Bending stresses associated with regional isostasy dominate the stress field. This is denoted by extensional stresses (red) overlying compression (blue) in the region of the inner valley ($x < 15$ km) and compression overlying extension in the region of the flanking mountains ($x > 20$ km). Such bending results from isostatic plate flexure in compensation of the axial valley (Lin and Parmentier, 1990; Thatcher and Hill, 1995). (3) A nominal amount of horizontal extensional stress exists because stretching of the lithosphere was not perfectly accommodated by normal faulting. This is evident by a shift of stresses toward extension (red) in the region. (4) The active normal fault induces a nominal amount of local stresses near its base (yellow/red region beneath the 750 °C contour).

When an active center becomes extinct, the sea-floor spreading ceases and so does the steady-state lithospheric stretching rate, V_{ext}. With no steady-state stretching, would the lithosphere relax enough to remove a significant portion of the axial valley? We have developed a model for an extinct center that incorporates the following features. (1) The steady-state topography and stresses of an active center (i.e., Fig. 3a) are used as initial conditions for the extinct center model. (2) No strain rate is applied to the lithosphere on the right side of the model. (3) The innermost rift-bounding fault remains a frictionless sliding plane. (4) Crustal and mantle temperatures are allowed to cool down according to models of conductive heat transfer, leading to gradual increases in the viscosities of the crust and mantle. (5) Residual topography and stresses are allowed to relax with time in accordance with local viscosities.

We have calculated the changes in sea-floor topography and crustal and mantle stresses at various time steps following the extinction. Figure 3b shows the topography and horizontal deviatoric stress, $\sigma_x - P$, at 40 m.y. after extinction. Comparisons of the results of the active (Fig. 3a) and extinct (Fig. 3b) centers reveal that, to a first order, the relaxation process has insignificant influences on the overall axial valley topography and the stress field. Slight differences, however, do exist between the active and extinct centers. In Figure 3b, deviatoric stresses have diminished in the mantle, particularly at the base of the innermost normal fault. These changes are accompanied by a small (~50 m) normal faulting slip on the frictionless fault (Fig. 4b) and a reduction in overall horizontal extensional stresses (lesser red color in Fig. 3b) from the active center. Isostatic restoring forces have slightly raised both the axial valley and flanking mountains by a small amount (~100 m) relative to the seafloor far from the extinct center (Fig. 4, a and b). This isostatic response, however, occurs over too broad a region to significantly influence axial valley topography.

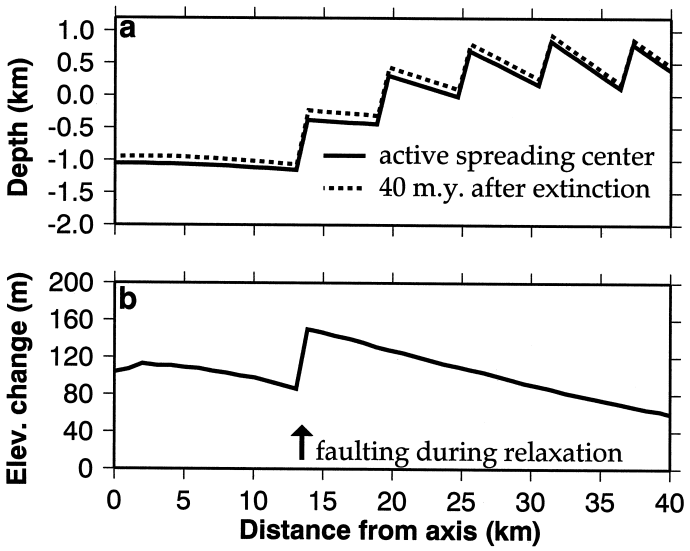

Figure 4. a: Comparison of predicted sea-floor topography of active and 40 m.y. old extinct centers (vertical exaggeration is 5:1). b: Elevation change from active to extinct center from a. Note that innermost fault undergoes small amount of normal faulting slip during relaxation process.

DISCUSSION

The axial valley associated with an active spreading center could potentially be removed by either of two specific mechanisms: (1) ductile relaxation of the lithosphere itself; or (2) reversal of motion on rift-bounding faults. The results of our models, however, suggest that the oceanic lithosphere near a slow-spreading center is too strong to allow significant ductile flow within the crust in tens of millions of years. On such a time scale, most of the deviatoric stresses within the crust and lithospheric mantle are predicted to be preserved. The temperature distribution that would be required to allow significant ductile flow of the crust may only be found near a fast-spreading center, where low viscosities prevent the formation of an axial valley (Chen and Morgan, 1990).

Our model also suggests that no obvious mechanism exists in which the rift-bounding normal faults can be reversed. In fact, extinction of a spreading center could lead to additional normal faulting either during the relaxation process (e.g., small normal faulting in Fig. 4b) or due to an increase in regional extensional strain rate if the extinction process is gradual (a reduction in the supply of magma could require a larger percentage of the half-spreading rate to be accommodated by normal faulting). The only way that faults could be reversed would be to introduce a compressional strain rate to the region immediately upon cessation of active spreading. Such a mechanism does not seem likely. Because conductive cooling increases lithospheric strength with time after extinction, should a compressional event occur long after extinction, a high level of com-

pressional stress would be required to reverse existing normal faults or to create new thrust faults.

The conclusion that axial valley topography is not significantly influenced by the relaxation process following extinction does not appear to be sensitive to model parameters. We adopted Shaw and Lin's cyclic faulting model as a base model for active spreading because it is self-consistent in the calculations of thermo-mechanical structure and fault kinematics. However, to minimize our reliance on any particular model, we have conducted extensive studies of other models with alternative choices of model parameters and starting topography. Examples of other modeling studies have considered effects of: (1) more than one rift-bounding normal fault active simultaneously; (2) variations in the locations and depths of both active and dormant faults; (3) different temperature cross sections; (4) alternative choices of rheological parameters; and (5) different applied strain rates. Though the details of the predicted topography and stresses vary between models, all of the studies support the main conclusion that lithosphere at a slow-spreading center has too high a viscosity to allow significant relaxation and no mechanisms exist to reverse rift-bounding normal faults.

CONCLUSIONS

We have simulated the evolution of a slow-spreading center upon cessation of active spreading in order to predict long-term changes in the axial valley. Results suggest that the axial valley created at a slow-spreading center persists because the crust is too strong to deform ductily and because no effective mechanism exists to reverse the topography created by rift-bounding normal faults. These conclusions do not appear to be sensitive to specific model parameters such as starting valley topography, rheology, or number of active faults. These results suggest that the persistence of axial valleys at extinct spreading centers is consistent with a lithospheric stretching model for active slow-spreading ridges.

ACKNOWLEDGMENTS

Supported by National Science Foundation grant OCE-9300708 (Lin) and Office of Naval Research grant N00014-91-J1433 (Lin and Shaw). We thank Javier Escartin for assistance in generation of Figure 1, William Shaw for providing the temperature profile used for viscosity calculations, and Don Forsyth, David Sandwell, Clem Chase, and an anonymous reader for thoughtful reviews. Woods Hole Oceanographic Institution contribution 8970.

REFERENCES CITED

Batiza, R., and Chase, C. G., 1981, Miocene spreading center south of Isla Guadalupe: Nature, v. 289, p. 787–789.

Blackman, D. K., and Forsyth, D. W., 1991, Isostatic compensation of tectonic features of the Mid-Atlantic Ridge 25°–27°30′S: Journal of Geophysical Research, v. 96, p. 11,741–11,758.

Chase, C. G., 1979, Asthenospheric counterflow: A kinematic model: Royal Astronomical Society Geophysical Journal, v. 56, p. 1–18.

Chen, Y., and Morgan, W. J., 1990, A nonlinear rheology model for mid-ocean ridge axis topography: Journal of Geophysical Research, v. 95, p. 17,583–17,604.

Collete, B. J., Verhoet, J., and de Mulder, A. F. J., 1980, Gravity and a model of the median valley: Journal of Geophysical Research, v. 47, p. 91–98.

Jonas, J., Hall, S., and Casey, J. F., 1991, Gravity anomalies over extinct spreading centers: A test of gravity models of active centers: Journal of Geophysical Research, v. 96, p. 11,759–11,777.

Kirby, S. H., 1983, Rheology of the lithosphere: Reviews of Geophysics, v. 21, p. 1458–1487.

Lin, J., and Bergman, E. A., 1990, Rift grabens, seismicity, and volcanic segmentation of the Mid-Atlantic Ridge: Kane to Atlantis fracture zones [abs.]: Eos (Transactions, American Geophysical Union), v. 71, p. 1572.

Lin, J., and Parmentier, E. M., 1989, Mechanisms of lithospheric extension at mid-ocean ridges: Geophysical Journal, v. 96, p. 1–22.

Lin, J., and Parmentier, E. M., 1990, A finite amplitude necking model of rifting in brittle lithosphere: Journal of Geophysical Research, v. 95, p. 4909–4923.

Lin, J., Purdy, G. M., Schouten, H., Sempere, J. C., and Zervas, C., 1990, Evidence from gravity data for focused magmatic accretion along the Mid-Atlantic Ridge: Nature, v. 344, p. 627–632.

Louden, K. E., White, R. S., Potts, C. G., and Forsyth, D. W., 1986, Structure and seismotectonics of the Vema Fracture Zone, Atlantic Ocean: Geological Society of London Journal, v. 143, p. 795–805.

Macdonald, K. C., 1982, Mid-ocean ridges: Fine scale tectonics, volcanic and hydrothermal processes within the plate boundary zone: Annual Review of Earth and Planetary Sciences, v. 10, p. 155–190.

Melosh, H. J., and Raefsky, A., 1981, A simple and efficient method for introducing faults into finite element computations: Seismological Society of America Bulletin, v. 71, p. 1391–1400.

Melosh, H. J., and Williams, C. A., 1989, Mechanics of graben formation in crustal rocks: A finite element analysis: Journal of Geophysical Research, v. 94, p. 13,961–13,973.

Neumann, G. A., and Forsyth, D. W., 1993, The paradox of the axial profile: Isostatic compensation along the axis of the Mid-Atlantic Ridge: Journal of Geophysical Research, v. 98, p. 17,891–17,910.

Osler, J. C., and Louden, K. E., 1995, Extinct spreading center in the Labrador Sea: Crustal structure from a two-dimensional seismic refraction velocity model: Journal of Geophysical Research, v. 100, p. 2261–2278.

Parmentier, E. M., and Forsyth, D. W., 1985, Three-dimensional flow beneath a slow-spreading ridge axis: A dynamic contribution to the deepening of the median valley towards fracture zones: Journal of Geophysical Research, v. 90, p. 678–684.

Parmentier, E. M., and Oliver, J. E., 1979, A study of shallow global mantle flow due to the accretion and subduction of lithospheric plates: Royal Astronomical Society Geophysical Journal, v. 87, p. 155–171.

Phipps Morgan, J., and Chen, Y. J., 1993, Dependence of ridge-axis morphology on magma supply and spreading rate: Nature, v. 364, p. 706–708.

Phipps Morgan, J., Parmentier, E. M., and Lin, J., 1987, Mechanisms for the origin of mid-ocean ridge axial topography: Implications for the thermal and mechanical structure of accreting plate boundaries: Journal of Geophysical Research, v. 92, p. 12,823–12,836.

Purdy, G. M., and Detrick, R. S., 1986, The crustal structure of the Mid-Atlantic Ridge at 23 °N from seismic refraction studies: Journal of Geophysical Research, v. 91, p. 3739–3762.

Sandwell, D. T., and Smith, W. H. F., 1992, Global marine gravity from ERS-1, Geosat and Seasat reveals new tectonic fabric: Eos (Transactions, American Geophysical Union), v. 73, p. 133.

Shaw, P. R., and Lin, J., 1993, Causes and consequence of variations in faulting style at the Mid-Atlantic ridge: Journal of Geophysical Research, v. 98, p. 21,839–21,851.

Small, C., and Sandwell, D. T., 1994, Imaging mid-ocean ridge transitions with satellite gravity: Geology, v. 22, p. 123–126.

Solomon, S. C., Huang, P. Y., and Meinke, L., 1988, The seismic moment budget of slowly spreading ridges: Nature, v. 334, p. 58–60.

Tapponier, P., and Francheteau, J., 1978, Necking of the lithosphere and the mechanics of slowly accreting plate boundaries: Journal of Geophysical Research, v. 83, p. 3955–3970.

Thatcher, W., and Hill, D. P., 1995, A simple model for the fault-generated morphology of slow-spreading mid-ocean ridges: Journal of Geophysical Research, v. 100, p. 561–570.

Toomey, D. R., Solomon, S. C., and Purdy, G. M., 1988, Microearthquakes beneath the median valley of the Mid-Atlantic Ridge near 23 °N: Tomography and tectonics: Journal of Geophysical Research, v. 93, p. 9093–9112.

Manuscript received April 28, 1995
Revised manuscript received August 17, 1995
Manuscript accepted August 24, 1995

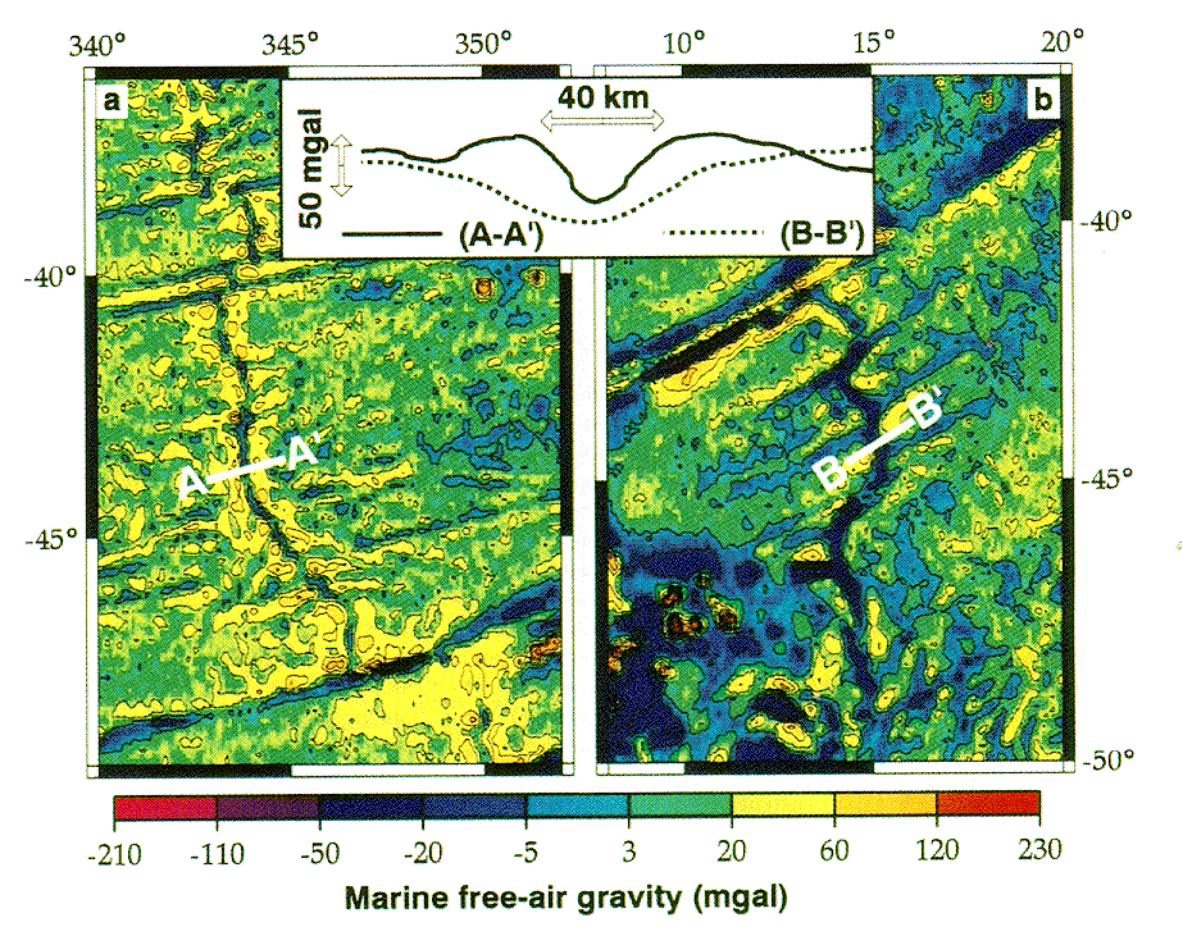
340°
345°
350°
10°
15°
20°
a
b
40 km
50 mgal
(A-A')
(B-B')
-40°
-45°
-50°
A
A'
B
B'
-210
-110
-50
-20
-5
3
20
60
120
230
Marine free-air gravity (mgal)

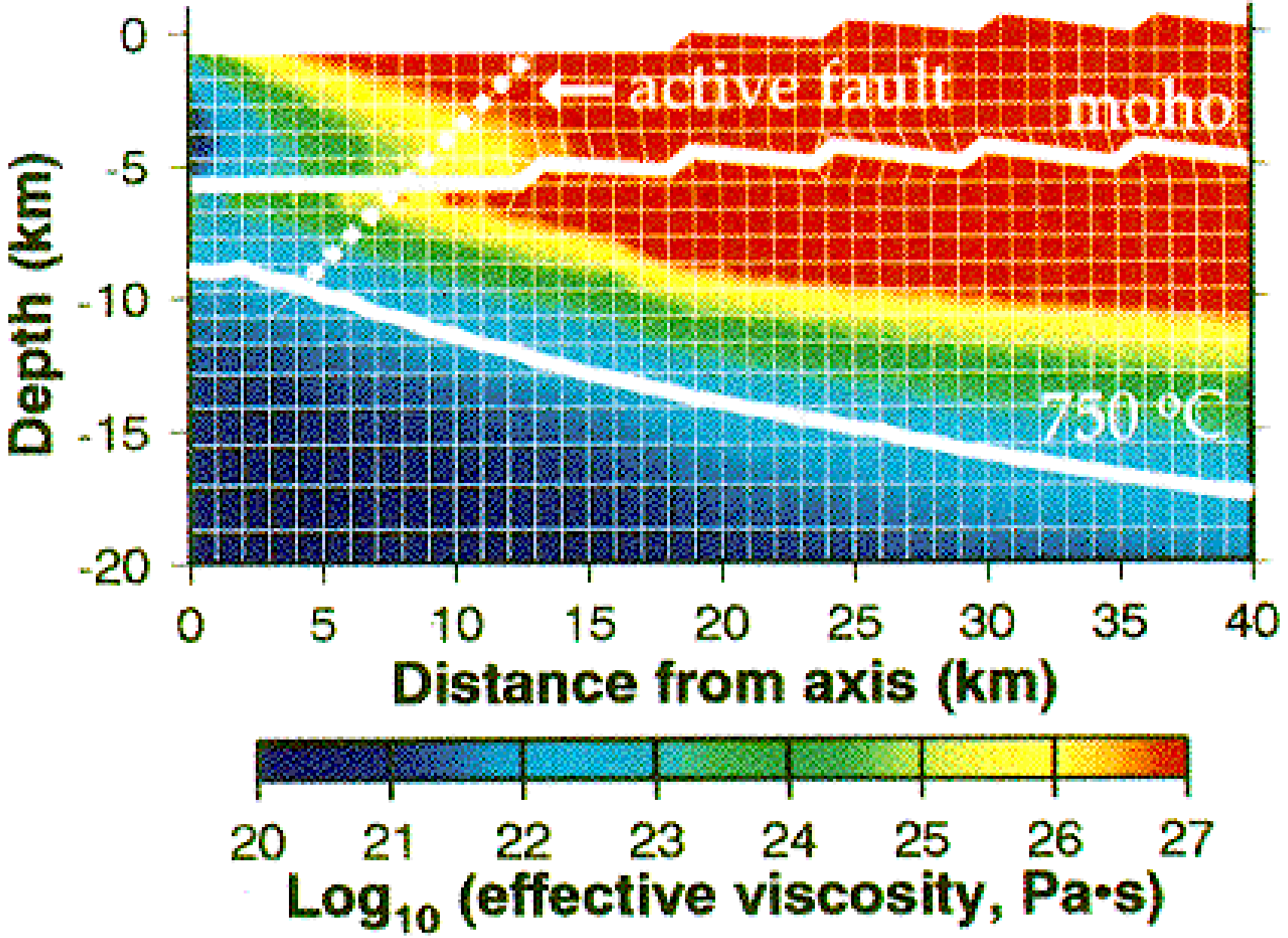
active fault
moho
750 °C
Depth (km)
0
-5
-10
-15
-20
0
5
10
15
20
25
30
35
40
Distance from axis (km)
20
21
22
23
24
25
26
27
Log10 (effective viscosity, Pa•s)

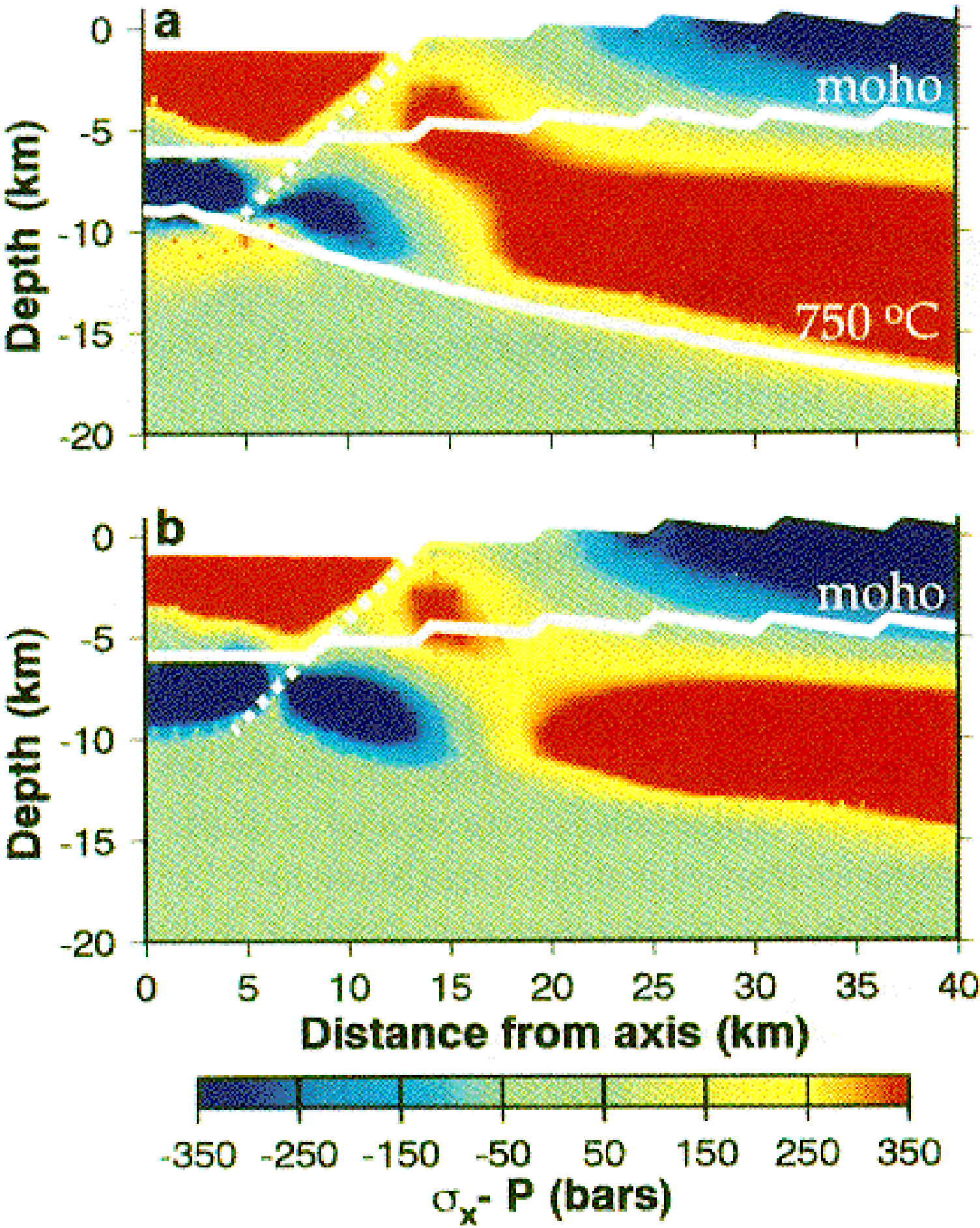
a
b
moho
moho
750 °C
Depth (km)
Depth (km)
0
-5
-10
-15
-20
0
5
10
15
20
25
30
35
40
Distance from axis (km)
-350
-250
-150
-50
50
150
250
350
σx- P (bars)